VIP NMR Spectroscopy Very Important Paper

Deutsche Ausgabe: DOI: 10.1002/ange.201605843
Internationale Ausgabe: DOI: 10.1002/anie.201605843

Enhancing the Sensitivity of CPMG Relaxation Dispersion to Conformational Exchange Processes by Multiple-Quantum Spectroscopy

*Tairan Yuwen, Pramodh Vallurupalli, and Lewis E. Kay**

Abstract: *A triple-quantum ^{1}H Carr–Purcell–Meiboom–Gill NMR relaxation dispersion experiment is presented that uses methyl group probes as reporters of conformational exchange in highly deuterated, methyl-protonated proteins. Significantly larger dispersion profiles, by as much as a factor of nine, can be obtained relative to single-quantum approaches, thus offering very significant advantages in applications involving interconverting conformers with only small changes in structure or in studies of rare states that are at very low populations. Applications to a number of protein systems are presented where the utility of the method, including its improved sensitivity to chemical exchange processes, is established.*

Protein conformational dynamics, leading to the exploration of states on the energy landscape with diverse biological activities, can be critically important for function.[1a,b] Often many of these states are sparsely populated and only transiently formed, challenging existing biophysical methods that are typically optimized for detailed studies of highly populated conformers.[2] Carr–Purcell–Meiboom–Gill (CPMG) relaxation dispersion NMR spectroscopy has emerged as a powerful approach for studies of such recalcitrant states by allowing the spectroscopist to "see the invisible" through spectra recorded of the highly populated ground state.[2,3] A series of data sets are measured that quantify the transverse relaxation of nuclei in the ground state, $R_{2,\mathrm{eff}}$, as a function of the rate of application of chemical shift refocusing pulses, ν_{CPMG}. For exchange processes occurring on the millisecond (ms) timescale, the resulting relaxation dispersion profiles are fit to extract populations of interconverting states and rates of interconversion as well as chemical-shift differences between ground and excited conformers.[2,3]

[*] Dr. T. Yuwen, Prof. L. E. Kay
Departments of Molecular Genetics, Biochemistry and Chemistry
University of Toronto
Toronto, Ontario M5S 1A8 (Canada)
E-mail: kay@pound.med.utoronto.ca
Dr. P. Vallurupalli
TIFR Centre for Interdisciplinary Sciences
21 Brundavan Colony, Narsingi, Hyderabad 500075 (India)
Prof. L. E. Kay
Hospital for Sick Children
Program in Molecular Structure and Function
555 University Avenue, Toronto, Ontario M5G 1X8 (Canada)
Supporting information and the ORCID identification number for an author of this article can be found under http://dx.doi.org/10.1002/anie.201605843.

Aside from the requirement that populations and rates be within a rather narrow window for observation of relaxation dispersion (typically rare state populations on the order of 1% or larger and exchange rates between several hundreds to several thousands per second), the chemical-shift differences ($\Delta\nu$) between exchanging conformers must be non-zero, and typically on the order of 25 Hz or larger. In applications where the populations of rare states are significantly lower than 1% or where similar conformers interconvert so that chemical-shift differences are small, the exchange process may escape detection. Studies at high static magnetic fields are helpful as chemical shifts scale linearly with the field, and the increase in the dispersion profile size is proportional to the square of the field in the limit where the rate of exchange is fast on the chemical-shift timescale.[3] A complementary approach involves measuring the decay of higher-order coherences during the CPMG relaxation element as these evolve as the sums of the chemical shifts of the individual component spins, thereby increasing the effective $\Delta\nu$ ($\Delta\nu_{\mathrm{eff}}$) and hence the size of the dispersion. Below, we illustrate the utility of one such experiment, by recording methyl ^{1}H CPMG profiles where triple quantum (TQ) ^{1}H coherences evolve during the CPMG element, scaling $\Delta\nu_{\mathrm{eff}}$ values by a factor of three relative to shift differences in related single quantum (SQ) experiments.[4] Thus, in cases where interconversion as probed by SQ coherences is in the fast-exchange limit, exchange involving TQ coherences may be in the intermediate regime so that populations and shift differences can be robustly extracted, while for other residues, exchange processes that were unobservable owing to a small $\Delta\nu$ in SQ CPMG applications become readily apparent. Furthermore, the increased sizes of the TQ dispersion profiles enable the study of exchange processes involving rare states at lower populations than would be possible by SQ approaches.

The ^{1}H TQ CPMG pulse schemes that have been developed for relaxation studies of highly deuterated $^{13}CH_3$-labeled proteins are illustrated in Figures 1A and in the Supporting Information, Figure S1. Protein deuteration is critical in these experiments to eliminate homonuclear scalar couplings with methyl protons, which would otherwise lead to pathologic dispersion profiles.[5] Fortunately, robust methods exist for the preparation of methyl-protonated, highly deuterated proteins,[6] with the utility of this labeling demonstrated in many protein applications.[7a,b] Central to the sequence is the CPMG relaxation element during which variable numbers of refocusing pulses are applied and where the coherences of interest at the start are given by $3C_zI^1_+I^2_+I^3_+ + 3C_zI^1_-I^2_-I^3_-$ when the phase cycle is taken into account, with C_z and $I^j_\pm = I^j_x \pm iI^j_y$ denoting ^{13}C longitudinal

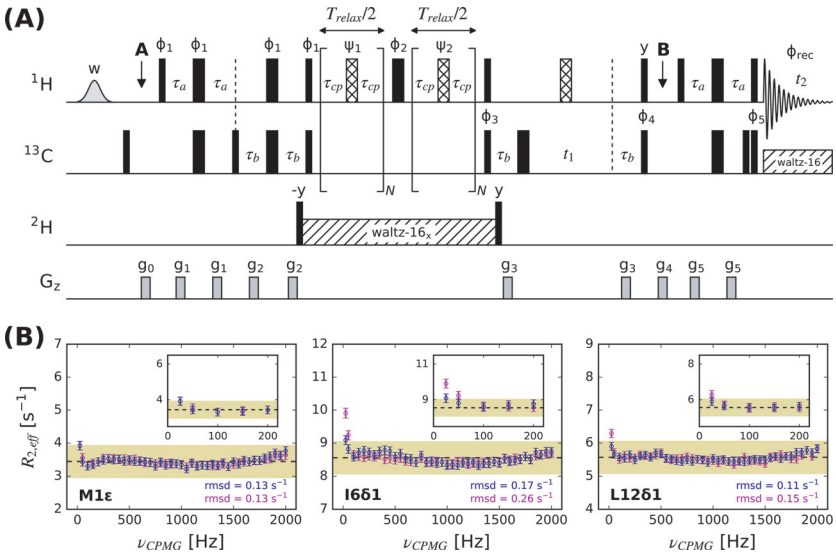

Figure 1. A) Pulse scheme for the measurement of methyl ^{1}H TQ CPMG relaxation dispersion profiles using highly deuterated, $^{13}CH_3$-labeled protein samples. Details are given in the Supporting Information. B) Profiles for selected methyl groups of GB1 recorded without (magenta) or with (blue) ^{2}H decoupling during the 40 ms CPMG interval are shown, 600 MHz, 25 °C. The $R_{2,eff}$ rates are corrected for differential relaxation of antiphase and in-phase ^{1}H TQ coherences, as described in the Supporting Information [Eq. (S7)]. Spurious $R_{2,eff}$ values are noted for most residues for $\nu_{CPMG} = 25$ Hz when ^{2}H decoupling is not applied (see text); these decrease significantly with decoupling. Note that in the absence of decoupling, these spurious rates are largest for Ile (2 deuterons on the carbon adjacent to $^{13}C^{\delta1}$), followed by Leu and Val (1 deuteron). RMSD values between $R_{2,eff}$ and the best-fit horizontal lines are indicated; the average RMSD is 0.20 ± 0.07 s^{-1}, which is approximately half the value measured in the absence of decoupling, and largely the result of elevated $R_{2,eff}(\nu_{CPMG} = 25$ Hz) rates. Yellow bars denote RMSD ± 0.5 s^{-1}, with insets showing expanded regions of the profiles.

and ^{1}H transverse magnetization, respectively, and 1, 2, and 3 are labels for the three equivalent methyl ^{1}H spins. Although there is a sensitivity penalty to pay for the TQ selection, it is modest. For example, a pulse scheme that selects double quantum (DQ) coherences loses half its sensitivity by eliminating the zero quantum component. By extension, one might assume that only one quarter of the methyl signal remains when the TQ terms are chosen. In fact, 3/4 of the signal is preserved when relaxation is neglected. This can be understood by noting that at the start of the CPMG interval, and considering the first line of the phase cycle (see the Supporting Information), the terms of interest are given by $8C_zI^1_xI^2_yI^3_y + 8C_zI^1_yI^2_xI^3_y + 8C_zI^1_yI^2_yI^3_x = 8C_zQ$. The Cartesian operators can be replaced by $I^j_\pm$ to show that $8C_zQ$ consists exclusively of TQ and SQ elements. TQ selection (phase cycling, Figure 1) preserves only those terms of the form $3C_zI^1_+I^2_+I^3_+$, $3C_zI^1_-I^2_-I^3_-$ that then evolve during the CPMG period. In order to follow how these TQ elements are subsequently transferred back to observable ^{1}H magnetization by the remainder of the pulse scheme, it is convenient to recast them in terms of Cartesian operators. It can then be shown that $6C_zQ$ of the initial $8C_zQ$ is ultimately detected, corresponding to 3/4 of the starting signal (see the Supporting Information).

As the ^{1}H coherences in the TQ elements contain both x and y magnetization components, a ^{1}H CPMG scheme must be employed that can efficiently refocus both transverse elements. Simulations and experiments have established that this can be achieved if the phase of each successive composite ^{1}H 180° pulse during the CPMG interval is incremented according to the XY-16 recipe.[8] This is illustrated in Figure 1B, where an application to a [U-^{2}H;Ileδ1-$^{13}CH_3$;Leu,Val-$^{13}CH_3$/$^{12}CD_3$;Met-$^{13}CH_3$]-labeled (ILVM-$^{13}CH_3$ labeled) B1 domain from immunoglobulin binding protein G (GB1) is presented. GB1 shows little evidence of conformational exchange in other experiments so that flat dispersion profiles would be expected in the ^{1}H TQ CPMG profiles as well. Indeed, these are obtained, but only when low-power ^{2}H decoupling is used during the CPMG element (blue curves). This minimizes the effects of small three-bond ^{2}H methyl–^{1}H couplings, which otherwise give rise to elevated ^{1}H $R_{2,eff}$ rates for small ν_{CPMG} values (< 100 Hz), from a scalar relaxation of the second kind mechanism.[9]

It is important to note that the antiphase TQ elements present at the start of the CPMG period, $3C_zI^1_+I^2_+I^3_+ + 3C_zI^1_-I^2_-I^3_-$, interconvert with in-phase TQ terms, $-1.5iI^1_+I^2_+I^3_+ + 1.5iI^1_-I^2_-I^3_-$, through one-bond ^{1}H–^{13}C scalar-coupled evolution that occurs during the intervals between ^{1}H refocusing pulses. As described in the Supporting Information, we have calculated the difference in relaxation rates between in-phase ($R_{2,I}$) and antiphase ($R_{2,A}$) elements, $\Delta R_2 = R_{2,I} - R_{2,A}$, to be $\Delta R_2 = 0.3d^2_{CH}[3J(\omega_c) + 6K(\omega_c)]$; d_{CH} and the auto- ($J(\omega_c)$) and cross- ($K(\omega_c)$) correlation spectral-density functions are defined in the Supporting Information, and ω_C is the ^{13}C Larmor frequency. This resulting imbalance between relaxation rates can lead to small errors in the dispersion profiles[10] that are easily corrected so long as ΔR_2 is known or by including ΔR_2 as a fitting parameter in the analysis of the dispersion profiles (see the Supporting Information).

Having established that essentially flat profiles are obtained in cases where millisecond timescale dynamics are not present, we next investigated an FF domain that has previously been shown to interconvert between a natively folded state and an on-pathway folding intermediate.[11] Figure 2 A–C shows a comparison of the methyl ^{1}H dispersion curves for Met40 ε (A), Ile44 δ1 (B), and Leu55 δ1 (C) measured on an ILVM-$^{13}CH_3$-labeled sample with the scheme of Figure 1A and on an ILVM-$^{13}CHD_2$-labeled sample ([U-^{2}H;Ileδ1-$^{13}CHD_2$;Leu,Val-$^{13}CHD_2$/$^{13}CHD_2$;Met-$^{13}CHD_2$]) using a previously published SQ experiment that is of high sensitivity and optimized for $^{13}CHD_2$ methyl probes.[12] As discussed below, it is also possible to measure ^{1}H SQ profiles using $^{13}CH_3$-labeled samples so long as care is taken to select ^{1}H magnetization exclusively from the two 1/2 manifolds, eliminating contributions from the 3/2 manifold.[13] This

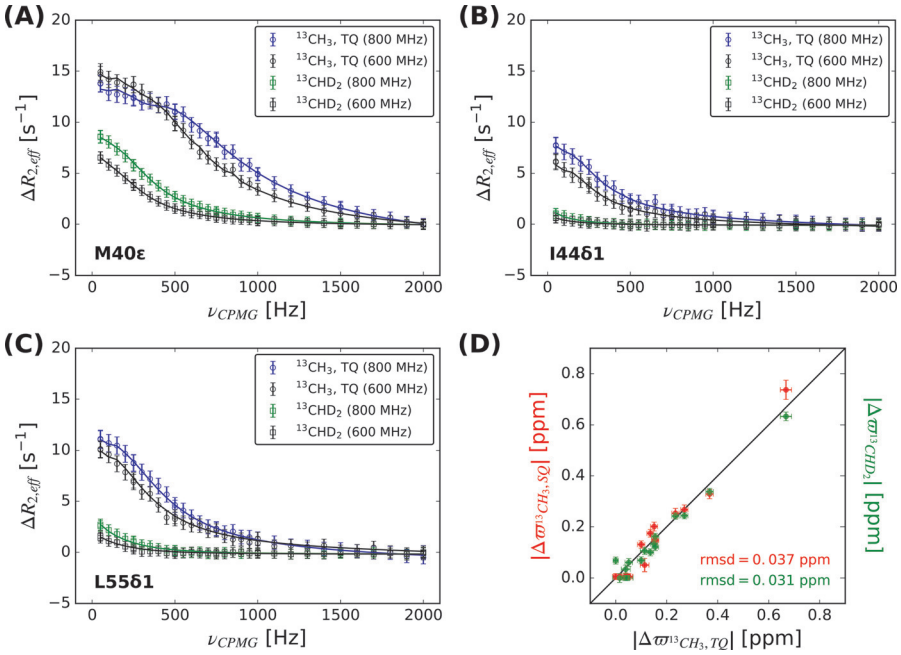

Figure 2. A–C) ^{1}H TQ and SQ CPMG relaxation dispersion profiles, $\Delta R_{2,eff} = R_{2,eff} - R_{2,eff}(\nu_{CPMG} = 2\text{ kHz})$, of selected residues from highly deuterated FF domains,[11] labeled as ILVM-$^{13}CH_3$ (TQ) or ILVM-$^{13}CHD_2$ (SQ), 800 and 600 MHz, 25 °C. Experimental data points are indicated by circles and squares and were fit to a two-site exchange model (solid lines, see the Supporting Information). Data recorded at 600 and 800 MHz and from all residues with dispersion profiles $> 3\text{ s}^{-1}$ (SQ) or 7 s^{-1} (TQ) were fit simultaneously, as described in the Supporting Information. D) Linear correlation of extracted $\Delta\varpi$ values (ppm) from TQ (*x* axis) and SQ profiles (*y* axis, either $^{13}CH_3$ (red) or $^{13}CHD_2$ (green)). The pulse schemes used to record the $^{13}CH_3$ and $^{13}CHD_2$ SQ CPMG data sets have been described previously.[12,15]

greatly suppresses artifacts that arise from inevitable CPMG pulse imperfections that lead to interchange between fast and slowly relaxing ^{1}H transitions and consequently the generation of pathologic dispersion profiles.[13] However, there is a steep price in sensitivity to be paid, leading to poorer quality profiles than those obtained from the $^{13}CHD_2$ methyl experiment (see below). In Figure 2 A–C, $\Delta R_{2,eff} = R_{2,eff} - R_{2,eff}(\nu_{CPMG} = 2\text{ kHz})$ is plotted so that the difference between the TQ and SQ dispersion profiles can be fully appreciated. In the case of M40, the timescale of the exchange process has been significantly reduced in the TQ experiment, which can be seen from the initial portion of the $\Delta R_{2,eff}$ versus ν_{CPMG} profile where $\Delta R_{2,eff}$ is relatively flat, whereas for the SQ curve, $\Delta R_{2,eff}$ decreases more rapidly with ν_{CPMG}. Notably, although for the I44δ1 methyl group the SQ dispersion curve is essentially flat, $R_{ex} = R_{2,eff}(\nu_{CPMG} = 25\text{ Hz}) - R_{2,eff}(\nu_{CPMG} = 2\text{ kHz}) \approx 1\text{ s}^{-1}$, and the R_{ex} value for the TQ profile is about 7.5 s^{-1}. Thus, I44δ1 would not be included in the set of methyl groups sensitive to conformational exchange in an analysis of SQ CPMG data, although it is clear from the TQ data set that I44 is a reporter of millisecond exchange dynamics. In total, dispersion profiles for only five methyl groups with $R_{ex} \geq 3\text{ s}^{-1}$ (800 MHz) were obtained in the SQ data set, whereas ten methyl groups with exchange contributions exceeding 7 s^{-1} (800 MHz) were measured from the TQ experiment. These were fit to a two-site model of chemical exchange, $G \underset{k_{EG}}{\overset{k_{GE}}{\rightleftharpoons}} E$, to extract the population of the rare state, p_E, and the exchange rate, $k_{ex} = k_{GE} + k_{EG}$. Values of $(p_E, k_{ex}) = (0.95 \pm 0.02\,\%,\ 1600 \pm 50\text{ s}^{-1})$, $(1.2 \pm 0.01\,\%,\ 1440 \pm 20\text{ s}^{-1})$, and $(1.1 \pm 0.03\,\%,\ 1590 \pm 60\text{ s}^{-1})$ were obtained from independent fits of the TQ, SQ ($^{13}CHD_2$), and SQ ($^{13}CH_3$) data, respectively, which are in reasonably good agreement. Notably, the $\Delta\varpi$ values extracted from fits of the TQ and SQ ^{1}H CPMG data sets are in excellent agreement (Figure 2 D), taking into account the threefold increase in $\Delta\nu$ for the TQ profiles.

As described above, the TQ experiment significantly decreases the timescale of the chemical exchange process, which is equivalent to increasing the static magnetic field by a factor of three. The exchange timescale can be quantified[14] by the parameter $\alpha = 2(k_{ex}/\Delta\omega)^2/(1 + (k_{ex}/\Delta\omega)^2)$, which ranges from 0 (slow exchange) to 2 (fast exchange); α values are given on a per-residue basis for the FF domain in Figure 3 A (800 MHz). The

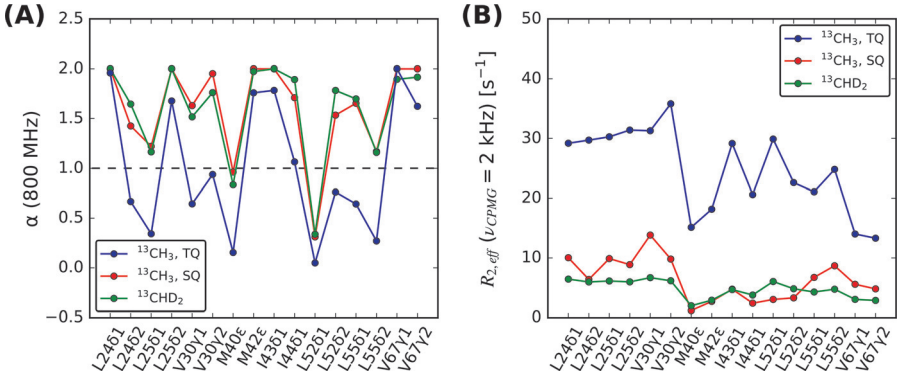

Figure 3. A) Plot of α, quantifying the chemical-shift exchange timescale versus residue for the FF domain, 800 MHz, 25 °C, as calculated from Eq. (14) of Millet et al.[14] (formula given in the text). The values of p_E, k_{ex}, and $\Delta\varpi$ for the calculation were obtained from global fits of TQ (blue) or SQ (red, green) dispersion profiles. In the latter case, the SQ dispersion profiles were measured either on $^{13}CH_3$ (red) or $^{13}CHD_2$ (green) labeled samples. B) Comparison of the $R_{2,eff}(\nu_{CPMG} = 2\text{ kHz})$ rates for residues of the FF domain (600 MHz, 25 °C), illustrating significantly larger transverse relaxation times for ^{1}H TQ (blue) relative to ^{1}H SQ (red, green) coherences.

considerable advantage for the TQ ^{1}H CPMG experiment with respect to the size of the dispersion profiles, illustrated in Figure 2 A–C, is offset somewhat by the increase in relaxation rates for TQ coherences relative to SQ magnetization (Figure 3 B). For applications to relatively small proteins, this is not likely to be a major deterrent but studies of larger proteins would benefit from labeling only one or two methyl types at a time so as to decrease relaxation contributions from external proton sources.

We were interested in comparing the relative sensitivities of different ^{1}H CPMG experiments, in particular because our previous ^{1}H CPMG scheme for $^{13}CH_3$-labeled proteins was of such low signal-to-noise (SN) ratio. We obtained relative SN ratios for correlations in TQ and SQ experiments recorded on the ILVM-$^{13}CH_3$-labeled FF domain and for a SQ data set measured on an ILVM-$^{13}CHD_2$ sample (Figure S2), with T_{relax} set to 0. As expected, the $^{13}CH_3$ SQ experiment[15] is very insensitive, approximately 20-fold less than a 2D HMQC data set, whereas the SN ratios of correlations in the corresponding TQ experiment increased by roughly a factor of ten, to approximately one half that obtained in the reference HMQC. Cross-peaks in the $^{13}CHD_2$ SQ CPMG data set are about 1.5-fold more sensitive for Leu and Val, and about 1.8-fold less sensitive for Ile and Met residues relative to those in the spectra generated from the TQ scheme. The significant differences between the Leu/Val and Ile/Met SN ratios reflect, in part, the fact that both isopropyl methyl groups of Leu and Val are $^{13}CHD_2$-labeled in the $^{13}CHD_2$ sample, whereas only one of the two methyl groups is $^{13}CH_3$ (the other $^{12}CD_3$) in the $^{13}CH_3$ sample,[16] thus increasing the sensitivity of the $^{13}CHD_2$-based experiment by a factor of two for Leu/Val simply on the basis of the label concentration (see the Supporting Information).

Figure 4 shows a comparison between the TQ and SQ profiles measured for a pair of Met residues in an [U-^{2}H;ILVM-$^{13}CH_3$]-labeled sample of the half proteasome[17] $\alpha_7\alpha_7$ (360 kDa), 50 °C. These Met residues are positioned at the N termini of each of the seven protomers in the barrel-like proteasome structure and are part of ten-residue disordered regions that form a primitive gate, covering the entrance pore of the proteasome.[18] Although significant profiles were observed in the TQ experiment, flat SQ ^{1}H dispersions were recorded for these residues. In a previous study using $^{13}CHD_2$ labeling, the SQ profiles were of much better SN, and small profiles were measured with R_{ex} values of 1.5 s^{-1} and 3 s^{-1} for M−1A and M1A, respectively.[12] This application further highlights the strength of the TQ scheme, where significantly larger dispersion profiles are typically recorded than for SQ-based experiments. In some studies, such as those involving proteasome gating, these differences can be critical.

In summary, we have presented a TQ ^{1}H CPMG experiment for probing conformational exchange in methyl-protonated, highly deuterated proteins. The experiment offers significant sensitivity gains over a previously published $^{13}CH_3$-based SQ scheme, but, equally important, significantly larger dispersion profiles are obtained, which can be essential for the quantification of exchange processes. As the size of the dispersion profile scales with the square of the chemical-shift difference between exchanging nuclei in the limit of fast exchange, the TQ profiles can be as much as nine times larger than the corresponding SQ curves. These larger dispersions can be "leveraged" to study exchange processes involving smaller rare-state populations than is possible in traditional SQ-based experiments. As such, the TQ CPMG approach provides a powerful avenue for studies of conformational exchange in systems undergoing structural rearrangements that would otherwise go undetected.

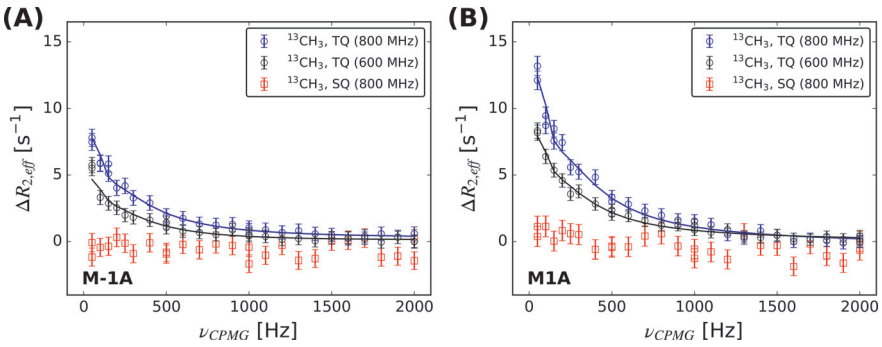

Figure 4. ^{1}H TQ (blue; 800 MHz; black; 600 MHz) and SQ (red, 800 MHz) CPMG relaxation dispersion profiles, $\Delta R_{2,eff}$, of Met residues at positions −1 and 1 of the half proteasome, $\alpha_7\alpha_7$, which are part of the N-terminal gating residues localized to the "out" position above the proteasome barrel (referred to as M−1A and M1A, respectively).[18] The dispersion profiles were measured on a 0.9 mM sample of ILVM $^{13}CH_3$-$\alpha_7\alpha_7$, 50 °C, using the pulse scheme of Figure 1 and a previously published SQ experiment for $^{13}CH_3$-labeled methyl groups.[13] The ^{1}H TQ(SQ) $R_{2,eff}(\nu_{CPMG}=2\text{ kHz})$ rates are 9.5 s^{-1} (ca. 1 s^{-1}) and 17.8 s^{-1} (ca. 2 s^{-1}) for M−1A and M1A, respectively.

Acknowledgements

This work was funded through a Canadian Institute of Health Research grant to L.E.K. L.E.K. holds a Canada Research Chair in Biochemistry. We are grateful to Dr. Ranjith Muhandiram and Dr. Ashok Sekhar for useful discussions.

Keywords: conformational dynamics · isotopic labeling · NMR spectroscopy · proteins

How to cite: *Angew. Chem. Int. Ed.* **2016**, *55*, 11490–11494
Angew. Chem. **2016**, *128*, 11662–11666

[1] a) K. Henzler-Wildman, D. Kern, *Nature* **2007**, *450*, 964–972; b) M. Karplus, J. Kuriyan, *Proc. Natl. Acad. Sci. USA* **2005**, *102*, 6679–6685.
[2] A. Sekhar, L. E. Kay, *Proc. Natl. Acad. Sci. USA* **2013**, *110*, 12867–12874.
[3] A. G. Palmer, C. D. Kroenke, J. P. Loria, *Methods Enzymol.* **2001**, *339*, 204–238.
[4] G. Bodenhausen, *Prog. Nucl. Magn. Reson. Spectrosc.* **1980**, *14*, 137–173.
[5] R. Ishima, D. Torchia, *J. Biomol. NMR* **2003**, *25*, 243–248.

[6] V. Tugarinov, L. E. Kay, *J. Biomol. NMR* **2004**, *28*, 165 – 172.
[7] a) R. Rosenzweig, L. E. Kay, *Annu. Rev. Biochem.* **2014**, *83*, 291 – 315; b) I. Gelis, A. M. Bonvin, D. Keramisanou, M. Koukaki, G. Gouridis, S. Karamanou, A. Economou, C. G. Kalodimos, *Cell* **2007**, *131*, 756 – 769.
[8] T. Gullion, D. B. Baker, M. S. Conradi, *J. Magn. Reson.* **1990**, *89*, 479 – 484.
[9] A. Abragam, *Principles of Nuclear Magnetism*, Clarendon Press, Oxford, **1961**.
[10] J. P. Loria, M. Rance, A. G. Palmer, *J. Am. Chem. Soc.* **1999**, *121*, 2331 – 2332.
[11] D. M. Korzhnev, T. L. Religa, W. Banachewicz, A. R. Fersht, L. E. Kay, *Science* **2010**, *329*, 1312 – 1316.
[12] A. J. Baldwin, T. L. Religa, D. F. Hansen, G. Bouvignies, L. E. Kay, *J. Am. Chem. Soc.* **2010**, *132*, 10992 – 10995.
[13] V. Tugarinov, L. E. Kay, *J. Am. Chem. Soc.* **2007**, *129*, 9514 – 9521.
[14] O. Millet, J. P. Loria, C. D. Kroenke, M. Pons, A. G. Palmer, *J. Am. Chem. Soc.* **2000**, *122*, 2867 – 2877.
[15] V. Tugarinov, L. E. Kay, *J. Am. Chem. Soc.* **2006**, *128*, 7299 – 7308.
[16] V. Tugarinov, L. E. Kay, *ChemBioChem* **2005**, *6*, 1567 – 1577.
[17] R. Sprangers, L. E. Kay, *Nature* **2007**, *445*, 618 – 622.
[18] T. L. Religa, R. Sprangers, L. E. Kay, *Science* **2010**, *328*, 98 – 102.

Received: June 16, 2016
Published online: August 16, 2016

